![cancers logo] *cancers*

MDPI

Article

^{18}F-FDG-PET Can Predict Microvessel Density in Head and Neck Squamous Cell Carcinoma

Alexey Surov [1],* , **Hans Jonas Meyer [1]**, **Anne-Kathrin Höhn [2]**, **Andreas Wienke [3]** ,
Osama Sabri [4] and Sandra Purz [4]

[1] Department of Diagnostic and Interventional Radiology, University Hospital of Leipzig, Liebigstrasse 20, 04103 Leipzig, Germany; hans-jonas.meyer@medizin.uni-leipzig.de
[2] Department of Pathology, University Hospital of Leipzig, Liebigstrasse 20, 04103 Leipzig, Germany; Annekathrin.hoehn@medizin.uni-leipzig.de
[3] Institute of Medical Epidemiology, Biostatistics, and Informatics, Martin-Luther-University Halle-Wittenberg, Magdeburger Str. 8, 06097 Halle, Germany; andreas.wienke@uk-halle.de
[4] Department of Nuclear Medicine, University Hospital of Leipzig, Liebigstrasse 18, 04103 Leipzig, Germany; Osama.Sabri@medizin.uni-leipzig.de (O.S.); sandra.purz@medizin.uni-leipzig.de (S.P.)
* Correspondence: Alexey.Surov@medizin.uni-leipzig.de

![check for updates]

Abstract: *Aim*: Positron emission tomography (PET) with ^{18}F-fluordeoxyglucose (^{18}F-FDG) plays an essential role in the staging and tumor monitoring of head and neck squamous cell carcinoma (HNSCC). Microvessel density (MVD) is one of the clinically important histopathological features in HNSCC. The purpose of this study was to analyze possible associations between ^{18}F-FDG-PET findings and MVD parameters in HNSCC. *Materials and Methods*: Overall, 22 patients with a mean age of 55.2 ± 11.0 and with different HNSCC were acquired. In all cases, whole-body ^{18}F-FDG-PET was performed. For each tumor, the maximum and mean standardized uptake values (SUV_{max}; SUV_{mean}) were determined. The MVD, including stained vessel area and total number of vessels, was estimated on CD105 stained specimens. All specimens were digitalized and analyzed by using ImageJ software 1.48v. Spearman's correlation coefficient (r) was used to analyze associations between investigated parameters. *p*-values of <0.05 were taken to indicate statistical significance. *Results:* SUV_{max} correlated with vessel area ($r = 0.532$, $p = 0.011$) and vessel count ($r = 0.434$, $p = 0.043$). Receiver operating characteristic analysis identified a threshold SUV_{max} of 15 to predict tumors with high MVD with a sensitivity of 72.7% and specificity of 81.8%, with an area under the curve of 82.6%. *Conclusion:* ^{8}F-FDG-PET parameters correlate statistically significantly with MVD in HNSCC. SUV_{max} may be used for discrimination of tumors with high tumor-related MVD.

1. Introduction

Radiological imaging, especially positron emission tomography (PET) with ^{18}F-fluorodeoxyglucose (^{18}F-FDG), plays an essential role in characterization head and neck squamous cell carcinoma (HNSCC). ^{18}F-FDG-PET is increasingly used for the staging and treatment monitoring of HNSCC [1–3]. As reported previously, metabolic tumor activity measured via PET parameters such as maximum or mean standardized uptake values (SUV_{max} or SUV_{mean}) correlates well with tumor stage and grade [2,3]. Advanced T stage tumors show higher PET parameters like SUV_{max} and SUV_{mean} in comparison to T1/T2 tumors [2,3]. Similarly, poorly differentiated (G3) tumors have higher SUV_{max} than do low-grade (G1 or G2) lesions [3]. Furthermore, the metabolic tumor burden is associated with the clinical outcome of HNSCC: patients with high metabolic tumor

burden have been associated with higher distant metastasis rates, translating into worse survival [4,5]. In addition, ^{18}F-FDG-PET can also predict treatment success in HNSCC. It has been shown that SUV values can be used as biomarkers in predicting the therapy response in HNSCC [6,7]. Kitagawa et al. reported that the SUV of pre-treatment ^{18}F-FDG-PET is useful in predicting the response to treatment, and post-treatment ^{18}F-FDG-PET is valuable in predicting residual viable tumors. It was also mentioned that a lower SUV (<4) of post-treatment ^{18}F-FDG-PET was significantly correlated with good histological results after therapy [6].

Some reports indicated that ^{18}F-FDG-PET can reflect several clinically relevant histopathological features in HNSCC. So far, Jacob et al. found that SUV_{max} correlated statistically significantly with the proliferation index KI 67 ($r = 0.78$) and proliferating cell nuclear antigen ($r = 0.66$) [8]. Grönroos et al. showed that SUV_{max} tended to correlate with the expression of tumor suppressor protein p53 ($p = 0.47$, $p = 0.078$) [9]. Furthermore, SUV_{max} also correlated well with the expression of hypoxia-inducible factor HIF-1α [10]. It has also been shown that p16-positive tumors had lower SUV_{max} in comparison to p16-negative carcinomas [11,12].

According to the literature, microvessel density (MVD) also plays a significant role in HNSCC [13]. For example, MVD estimated from CD105 immunoexpression predicts a poor outcome in oral squamous cell carcinoma [13,14]. Like VEGF (vascular endothelial growth factor), CD105 (endoglin) is a hypoxia-inducible transmembrane glycoprotein, and its expression is up-regulated in actively proliferating endothelial cells. Endoglin has been described as a marker for tumor-related angiogenesis and neovascularization with potential in tumor diagnosis, prognosis, and therapy [15]. Xia et al. found that MVD can predict lymph node metastases and prognosis in HNSCC [16]. We assume that the parameters of ^{18}F-FDG-PET might also reflect MVD in HNSCC. However, no previous study has investigated the relationships between ^{18}F-FDG-PET and tumor MVD in HNSCC.

Therefore, the purpose of the present study was to analyze possible associations between ^{18}F-FDG-PET parameters and MVD in HNSCC.

2. Methods

This prospective study was approved by the institutional review board (Ethics Committee of the University of Leipzig, study codes 180-2007, 201-10-12072010, and 341-15-05102015). All methods were performed in accordance with the relevant guidelines and regulations. All patients gave their written informed consent.

2.1. Patients

For this study, patients with histologically proven HNSCC and available histopathological specimens and who underwent ^{18}F-FDG-PET/CT examinations at our institution were selected. Overall, there were 22 patients, 6 (26.1 %) women and 16 (73.9 %) men, with a mean age of 55.2 ± 11.0 years, age range of 24–77 years, and different HNSCC. Low-grade (G1/2) tumors were diagnosed in 10 cases (45.5%) and high-grade (G3) tumors in the remaining 12 (54.5%) patients.

2.2. Imaging

^{18}F-FDG-PET/CT

In all 22 patients, an ^{18}F-FDG-PET/CT (Siemens Biograph 16, Siemens Medical Solutions, Erlangen, Germany) was performed from the skull to the upper thigh after a fasting period of at least 6 h. Application of ^{18}F-FDG was performed intravenously with a body-weight-adapted dose (4 MBq/kg, range: 168–427 MBq, mean ± SD: 281 ± 62.2 MBq). PET/CT image acquisition started on average 76 min (range 60–90 min) after ^{18}F-FDG application. Low-dose CT was used for attenuation correction of the PET data.

The acquired PET/CT datasets were evaluated by a board-certified nuclear medicine practitioner and a board-certified radiologist with substantial PET/CT experience in oncological image interpretation.

PET/CT image analysis was performed on a dedicated workstation at Hermes Medical Solutions, Sweden. For each tumor, the maximum and mean SUV (SUV_{max}; SUV_{mean}) were determined from PET images (Figure 1). Prior to this, the tumor margins of the HNSCC were identified on CT images and fused PET/CT images, and a polygonal volume of interest (VOI) that include the entire lesion in the axial, sagittal, and coronal planes was placed in the PET dataset (SUV_{max} threshold 40%).
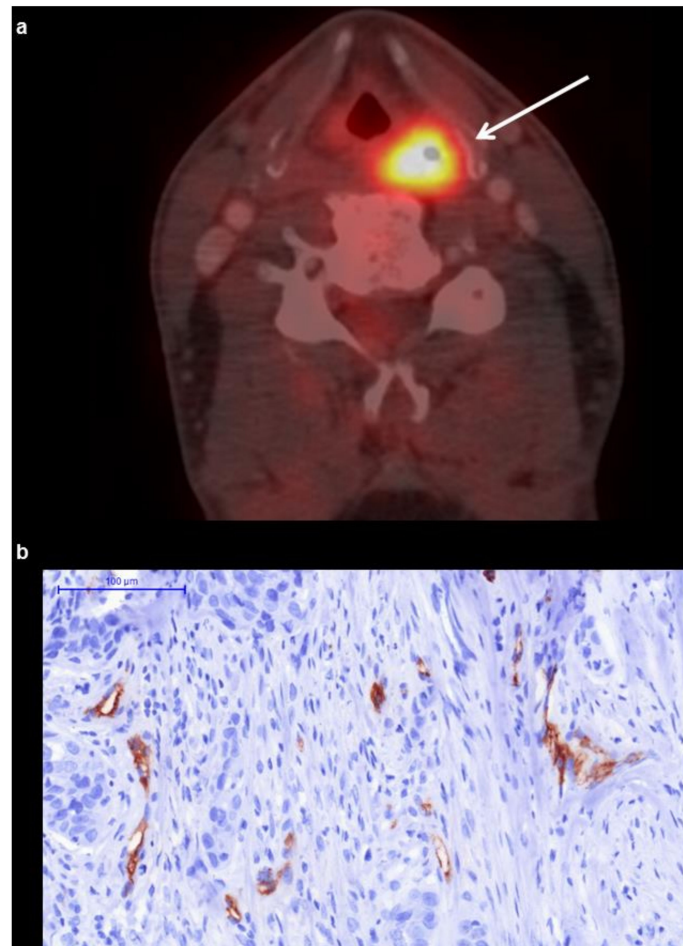

Figure 1. (**a**) ^{18}F-fluordeoxyglucose (^{18}F-FDG)-PET/CT shows a metabolically active hypopharyngeal lesion. The acquired ^{18}F-FDG-PET parameters of the lesion are as follows: maximum and mean standardized uptake values SUV_{max} = 22.07 and SUV_{mean} = 13.92. magnification: 200×. (**b**) Histopathological findings (CD 105 stained specimen). Vessel area is 1.2%, vessel count is 11.

2.3. Microvessel Density

In all cases, the diagnosis was confirmed histopathologically by tumor biopsy before any form of treatment. For the present study, the biopsy specimens were deparaffinized, rehydrated, and cut into 5 μm slices. The specimens were stained with CD 105 antigen (Abcamplc, 330 Cambridge Science Park, Cambridge, CB4 0FL, UK). Furthermore, all stained specimens were digitalized by using a Pannoramic microscope scanner (Pannoramic SCAN, 3DHISTECH Ltd., Budapest, Hungary) with Carl Zeiss objectives up to 41× bright field magnification by default. In the used bottom-up approach, the whole sample was acquired at high resolution. The digital slides (magnification of 200×) were evaluated using Pannoramic Viewer 1.15.4 (open source software, 3D HISTECH Ltd., Budapest, Hungary).

Thereafter, the digitalized histopathological images were analyzed using ImageJ software 1.48v (National Institutes of Health Image program) with a Windows system [17,18]. The microvessel density included the following parameters: stained vessel area (vessel area, % per high-power field), calculated

as the CD105 positive area divided by the total area of the analyzed histological specimens, and the total number of vessels (vessel count) according to Weidner et al. [19].

2.4. Statistical Analysis

Statistical analysis was performed using the SPSS package (IBM SPSS Statistics for Windows, version 22.0, Armonk, NY, USA: IBM corporation). The collected data were evaluated by means of descriptive statistics. The statistical data included means and medians with corresponding standard deviations and ranges of the acquired ^{18}F-FDG-PET and histopathological parameters.

Spearman's correlation coefficient (r) was used to analyze associations between the investigated variables. p-values of <0.05 were taken to indicate statistical significance. Furthermore, the sensitivity, specificity, negative and positive predictive values, accuracy, and area under the receiver operating characteristic curve (AUC) value were calculated for the diagnostic procedures. Thresholds were chosen to maximize the Youden index.

3. Results

Information regarding tumor localization, stage, and grade of the enrolled patients is given in Table 1. Table 2 shows a complete overview of the acquired ^{18}F-FDG-PET and histopathological parameters including mean values, standard deviations, and ranges.

Table 1. Clinical characteristics of the patients enrolled in the study.

No.	Sex	Age	Tumor Site	T Stage	N Stage	M Stage	Grading
1	female	33	Oral cavity	3	0	0	2
2	male	62	Larynx	3	3	0	3
3	male	55	Oropharynx	3	2	0	3
4	male	56	Hypopharynx	3	1	0	3
5	female	58	Oropharynx	1	2	0	3
6	male	24	Oral cavity	4	2	0	2
7	male	64	Oral cavity	2	1	0	3
8	male	57	Oropharynx	2	2	0	3
9	male	44	Larynx	4	0	0	3
10	female	77	Epipharynx	4	1	1	3
11	male	59	Oropharynx	3	1	0	2
12	male	53	Larynx	4	2	0	3
13	male	64	Hypopharynx	4	2	0	2
14	male	61	Oropharynx	4	2	0	2
15	male	58	Oropharynx	2	2	0	2
16	female	60	Oropharynx	4	2	0	4
17	male	55	Oropharynx	3	2	0	2
18	male	54	Oral cavity	4	2	0	2
19	female	65	Oropharynx	2	2	0	3
20	male	50	Oropharynx	2	2	0	3
21	male	48	Hypopharynx	2	2	0	2
22	female	58	Oral cavity	4	2	0	1

Table 2. Estimated ^{18}F-FDG-PET and microvessel density (MVD) parameters of head and neck squamous cell carcinoma (HNSCC).

Parameters	M ± SD	Median	Range
SUV_{max}	14.34 ± 5.05	14.79	5.9–24.1
SUV_{mean}	8.40 ± 3.11	8.28	3.63–14.87
Vessel Area	1.97 ± 1.15	1.76	0.4–4.56
Vessel Count	11.64 ± 4.97	10	5–25

SUV_{max} correlated statistically significantly with vessel area ($r = 0.532$, $p = 0.011$) and vessel count ($r = 0.434$, $p = 0.043$). SUV_{mean} also correlated statistically significantly with vessel area ($r = 0.465$, $p = 0.029$). In the next step, receiver operating characteristic (ROC) analysis was performed to predict tumors with high microvessel density (vessel area > 1.76% as a result of median split) using SUV_{max}. The Youden index identified a threshold SUV_{max} of 15 with a sensitivity of 72.7% and specificity of 81.8% (Figure 2). The positive predictive value was 80%, the negative predictive value was 75%, and the accuracy was 77.3%. The area under the curve was 82.6%.
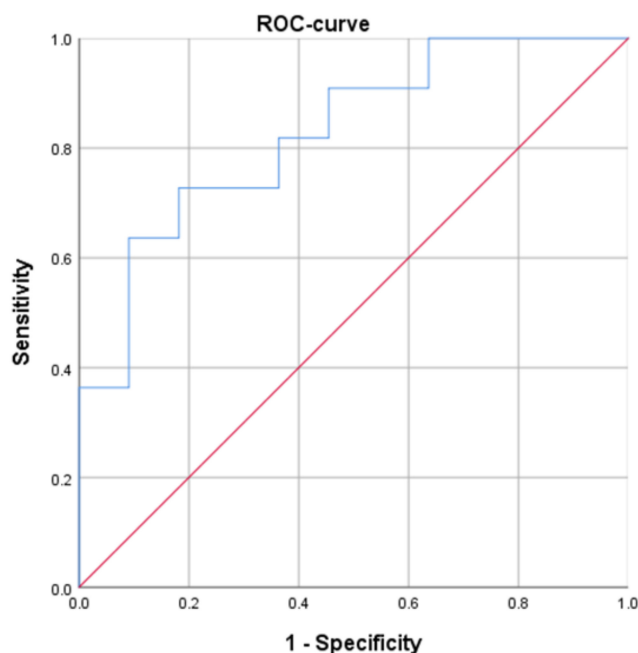

Figure 2. The receiver operating characteristic (ROC) curve using SUV_{max} for distinguishing tumors with high microvessel density from lesions with low microvascularization. The optimal threshold SUV_{max} is 15, resulting in a sensitivity of 70.0% and a specificity of 75.0%. The area under the curve is 82.6%.

4. Discussion

The present study identified significant associations between parameters of ^{18}F-FDG-PET and MVD in HNSCC. According to the literature, MVD is a very important histopathological feature in different malignancies. There are different immunohistochemical markers for the estimation of MVD. Some authors used pan-endothelial markers, namely, CD34, CD31, and von Willebrand factor [19–21]. However, it is well known that these markers have low sensitivity and specificity and are not always expressed in all intratumoral vessels [21]. In contrast to the non-specific pan-endothelial markers, CD105 or endoglin is upregulated in angiogenic vessels and accumulates preferentially in tumors [22,23]. Therefore, CD105 is a marker of tumor-related MVD.

Previously, numerous studies showed that CD105 correlated with tumor aggressiveness in lung cancer [24,25], breast carcinomas [26], colonic cancer [27], and endometrial carcinoma [28]. MVD is also one of the clinically relevant features in HNSCC [29–32]. According to the literature, tumor size/T stage correlated directly with the MVD/CD 105 ratio in oral cancers [31]. Furthermore, some reports indicated that high MVD/CD105 values were associated with the presence of lymph node metastasis in HNSCC [29,32,33]. Finally, high MVD/expression of CD105 was also associated with recurrence of disease or occurrence of distant metastasis and poorer 5-year survival [33–37]. Therefore, MVD can be applied as an important independent prognostic factor in HNSCC.

The possibility to predict MVD from imaging is very important. Previously, relationships between ^{18}F-FDG-PET findings and MVD were analyzed in several malignancies. Remarkably, different

correlation coefficients were observed between the investigated parameters. Furthermore, different markers for MVD were used. Han et al. used CD34 marker and did not observe statistically significant correlations between SUV_{max} and MVD in lung cancer [38]. However, Xing et al. also estimated MVD from CD 34 stained specimens and reported a very strong correlation between tumor MVD and SUV in lung cancer (r = 0.915, p < 0.01) [39]. In esophageal cancer, no significant correlations were detected between PET parameters and MVD measured from CD31 stained specimens [40]. Only few studies have analyzed the associations between PET and tumor-related MVD based on CD 105 expression. In the study by Groves et al., SUV_{max} correlated statistically significantly with MVD (r = 0.6, p = 0.005) in breast cancer [41]. Cochet et al. also investigated patients with breast cancer but could not identify statistically significant correlations between SUV_{max} and the expression of CD105 or CD34 [42]. However, interestingly, in the same study, SUV_{max} was associated with expression of CD105 in a non-triple-negative tumor subgroup (r = 0.5, p = 0.005) [42]. Finally, in colorectal cancer, no significant correlations between metabolic parameters (SUV_{max} or SUV_{mean}) and CD 105 expression were found [43].

In HNSCC, there have been no previous studies about associations between ^{18}F-FDG-PET and tumor-related MVD. The present study showed that SUV_{max} may predict MVD in HNSCC. Moreover, SUV_{max} may be used for discrimination of tumors with higher expression of CD 105, i.e., high-risk lesions. This finding is very important. It may help us to identify patients suitable for targeted therapy with anti-angiogenetic antibodies (e.g., anti-endoglin) in an oncological therapeutic setting. However, in agreement with the results by Groves et al. [41], the identified correlations were moderate. Also, the calculated negative and positive predictive values and the area under the curve and accuracy were relatively low. These facts limit the use of the present data to make a clinical decision.

Our study also identified another interesting aspect. The calculated correlation coefficients between SUV_{max} and MVD are comparable with those for specific perfusion parameters. In fact, as reported previously, one of the parameters of dynamic contrast-enhanced MRI, namely Kep, correlated with vessel area (r = 0.51, p = 0.041) in HNSCC [44]. Blood volume, a parameter of CT perfusion, correlated with vessel count (r = 0.59, p = 0.035) [45]. Furthermore, in the present study, we analyzed important tumor-related MVD estimated from CD 105 expression. Previous reports, however, investigated MVD using the expression of CD 31 or CD 34 [29,30]. According to the literature, these markers are not tumor-specific and do not play a clinical role in HNSCC [14,27]. The present study is limited due to a small number of patients. Clearly, further investigations with more cases are needed to verify our results.

5. Conclusions

^{18}F-FDG-PET parameters correlated statistically significantly with MVD in HNSCC. SUV_{max} may be used for discrimination of tumors with high tumor-related MVD.

Author Contributions: Conceptualization, A.S. and S.P.; methodology, S.P.; software, S.P., H.J.M. and A.-K.H.; validation, A.S., S.P. and O.S.; formal analysis, A.S.; investigation, S.P. and A.-K.H.; resources, H.J.M.; data curation, A.S.; writing—original draft preparation, A.S.; statistical analysis, A.W., writing—review and editing, S.P., O.S., A.W., H.J.M. and A.-K.H.; visualization, A.-K.H., H.J.M. and A.W.; supervision, S.P.; project administration, A.S.

Abbreviations

^{18}F-FDG	^{18}F-fluorodeoxyglucose
HNSCC	head and neck squamous cell carcinoma
MVD	micro vessel density
PET	positron emission tomography
ROC	receiver operating characteristic
SUV	standardized uptake values

References

1. Varoquaux, A.; Rager, O.; Poncet, A.; Delattre, B.M.; Ratib, O.; Becker, C.D.; Dulguerov, P.; Dulguerov, N.; Zaidi, H.; Becker, M. Detection and quantification of focal uptake in head and neck tumours: (18)F-FDG PET/MR versus PET/CT. *Eur. J. Nucl. Med. Mol. Imaging* **2014**, *41*, 462–475. [CrossRef]

2. Haerle, S.K.; Huber, G.F.; Hany, T.F.; Ahmad, N.; Schmid, D.T. Is there a correlation between 18F-FDG-PET standardized uptake value, T-classification, histological grading and the anatomic subsites in newly diagnosed squamous cell carcinoma of the head and neck? *Eur. Arch. Otorhinolaryngol.* **2010**, *267*, 1635–1640. [CrossRef] [PubMed]

3. Li, S.J.; Guo, W.; Ren, G.X.; Huang, G.; Chen, T.; Song, S.L. Expression of Glut-1 in primary and recurrent head and neck squamous cell carcinomas, and compared with 2-[18F]fluoro-2-deoxy-D-glucose accumulation in positron emission tomography. *Br. J. Oral Maxillofac. Surg.* **2008**, *46*, 180–186. [CrossRef]

4. Kim, S.Y.; Roh, J.L.; Kim, J.S.; Ryu, C.H.; Lee, J.H.; Cho, K.J.; Choi, S.H.; Nam, S.Y. Utility of FDG PET in patients with squamous cell carcinomas of the oral cavity. *Eur. J. Surg. Oncol.* **2008**, *34*, 208–215. [CrossRef] [PubMed]

5. Abgral, R.; Keromnes, N.; Robin, P.; Le Roux, P.Y.; Bourhis, D.; Palard, X.; Rousset, J.; Valette, G.; Marianowski, R.; Salaün, P.Y. Prognostic value of volumetric parameters measured by 18F-FDG PET/CT in patients with head and neck squamous cell carcinoma. *Eur. J. Nucl. Med. Mol. Imaging* **2014**, *41*, 659–667. [CrossRef] [PubMed]

6. Kitagawa, Y.; Sano, K.; Nishizawa, S.; Nakamura, M.; Ogasawara, T.; Sadato, N.; Yonekura, Y. FDG-PET for prediction of tumour aggressiveness and response to intra-arterial chemotherapy and radiotherapy in head and neck cancer. *Eur. J. Nucl. Med. Mol. Imaging* **2003**, *30*, 63–71. [PubMed]

7. Wong, K.H.; Panek, R.; Welsh, L.; Mcquaid, D.; Dunlop, A.; Riddell, A.; Murray, I.; Du, Y.; Chua, S.; Koh, D.M.; et al. The Predictive Value of Early Assessment After 1 Cycle of Induction Chemotherapy with 18F-FDG PET/CT and Diffusion-Weighted MRI for Response to Radical Chemoradiotherapy in Head and Neck Squamous Cell Carcinoma. *J. Nucl. Med.* **2016**, *57*, 1843–1850. [CrossRef] [PubMed]

8. Jacob, R.; Welkoborsky, H.J.; Mann, W.J.; Jauch, M.; Amedee, R. [Fluorine-18] Fluorodeoxyglucose Positron Emission Tomography, DNA Ploidy and Growth Fraction in Squamous-Cell Carcinomas of the Head and Neck. *ORL J. Otorhinolaryngol. Relat. Spec.* **2001**, *63*, 307–313. [CrossRef]

9. Grönroos, T.J.; Lehtiö, K.; Söderström, K.O.; Kronqvist, P.; Laine, J.; Eskola, O.; Viljanen, T.; Grénman, R.; Solin, O.; Minn, H. Hypoxia, blood flow and metabolism in squamous-cell carcinoma of the head and neck: Correlations between multiple immunohistochemical parameters and PET. *BMC Cancer* **2014**, *14*, 876. [CrossRef]

10. Zhao, K.; Yang, S.Y.; Zhou, S.H.; Dong, M.J.; Bao, Y.Y.; Yao, H.T. Fluorodeoxyglucose uptake in laryngeal carcinoma is associated with the expression of glucose transporter 1 and hypoxia inducible factor 1α and the phosphoinositide 3 kinase/protein kinase B pathway. *Oncol. Lett.* **2014**, *7*, 984–990. [CrossRef]

11. Surov, A.; Meyer, H.J.; Höhn, A.K.; Winter, K.; Sabri, O.; Purz, S. Associations Between [18F]FDG-PET and Complex Histopathological Parameters Including Tumor Cell Count and Expression of KI 67, EGFR, VEGF, HIF-1α, and p53 in Head and Neck Squamous Cell Carcinoma. *Mol. Imaging Biol.* **2019**, *21*, 368–374. [CrossRef]

12. Rasmussen, G.B.; Vogelius, I.R.; Rasmussen, J.H.; Schumaker, L.; Ioffe, O.; Cullen, K.; Fischer, B.M.; Therkildsen, M.H.; Specht, L.; Bentzen, S.M. Immunohistochemical biomarkers and FDG uptake on PET/CT in head and neck squamous cell carcinoma. *Acta Oncol.* **2015**, *54*, 1408–1415. [CrossRef]

13. Szafarowski, T.; Sierdzinski, J.; Szczepanski, M.J.; Whiteside, T.L.; Ludwig, N.; Krzeski, A. Microvessel density in head and neck squamous cell carcinoma. *Eur. Arch. Otorhinolaryngol.* **2018**, *275*, 1845–1851. [CrossRef]

14. Patil, B.R.; Bhat, K.; Somannavar, P.; Hosmani, J.; Kotrashetti, V.; Nayak, R. Comparison of immunohistochemical expression of vascular endothelial growth factor and CD105 in oral squamous cell carcinoma: Its correlation with prognosis. *J. Cancer Res. Ther.* **2018**, *14*, 421–427.

15. Nassiri, F.; Cusimano, M.D.; Scheithauer, B.W.; Rotondo, F.; Fazio, A.; Yousef, G.M.; Syro, L.V.; Kovacs, K.; Lloyd, R.V. Endoglin (CD105): A review of its role in angiogenesis and tumor diagnosis, progression and therapy. *Anticancer Res.* **2011**, *31*, 2283–2290.

16. Xia, X.; Du, R.; Zhao, L.; Sun, W.; Wang, X. Expression of AEG-1 and microvessel density correlates with metastasis and prognosis of oral squamous cell carcinoma. *Hum. Pathol.* **2014**, *45*, 858–865. [CrossRef]

17. Surov, A.; Stumpp, P.; Meyer, H.J.; Gawlitza, M.; Höhn, A.K.; Boehm, A.; Sabri, O.; Kahn, T.; Purz, S. Simultaneous 18F-FDG-PET/MRI: Associations between diffusion, glucose metabolism and histopathological parameters in patients with head and neck squamous cell carcinoma. *Oral Oncol.* **2016**, *58*, 14–20. [CrossRef]

18. Surov, A.; Meyer, H.J.; Winter, K.; Richter, C.; Hoehn, A.K. Histogram analysis parameters of apparent diffusion coefficient reflect tumor cellularity and proliferation activity in head and neck squamous cell carcinoma. *Oncotarget* **2018**, *9*, 23599–23607. [CrossRef]

19. Weidner, N.; Semple, J.P.; Welch, W.R.; Folkman, J. Tumor angiogenesis and metastasis—Correlation in invasive breast carcinoma. *N. Engl. J. Med.* **1991**, *324*, 1–8. [CrossRef]

20. Saad, R.S.; Liu, Y.L.; Nathan, G.; Celebrezze, J.; Medich, D.; Silverman, J.F. Endoglin (CD105) and vascular endothelial growth factor as prognostic markers in colorectal cancer. *Mod. Pathol.* **2004**, *17*, 197–203. [CrossRef]

21. Wang, J.M.; Kumar, S.; Pye, D.; Haboubi, N.; al-Nakib, L. Breast carcinoma: Comparative study of tumor vasculature using two endothelial cell markers. *J. Natl. Cancer Inst.* **1994**, *86*, 386–388. [CrossRef]

22. Duff, S.E.; Li, C.; Garland, J.M.; Kumar, S. CD105 is important for angiogenesis: Evidence and potential applications. *FASEB J.* **2003**, *17*, 984–992. [CrossRef]

23. Fonsatti, E.; Altomonte, M.; Nicotra, M.R.; Natali, P.G.; Maio, M. Endoglin (CD105): A powerful therapeutic target on tumor-associated angiogenetic blood vessels. *Oncogene* **2003**, *22*, 6557–6563. [CrossRef]

24. Brattstrom, D.; Bergqvist, M.; Wester, K.; Hesselius, P.; Ren, Z.P.; Scheibenpflug, L.; Wagenius, G.; Brodin, O. Endothelial markers and circulating angiogenic factors and p53 may be potential markers for recurrence in surgically resected nonsmall cell lung cancer patients. *Med. Sci. Monit.* **2004**, *10*, 331–338.

25. Mineo, T.C.; Ambrogi, V.; Baldi, A.; Rabitti, C.; Bollero, P.; Vincenzi, B.; Tonini, G. Prognostic impact of VEGF, CD31, CD34, and CD105 expression and tumour vessel invasion after radical surgery for IB-IIA non-small cell lung cancer. *J. Clin. Pathol.* **2004**, *57*, 591–597. [CrossRef]

26. Kumar, S.; Ghellal, A.; Li, C.; Byrne, G.; Haboubi, N.; Wang, J.M.; Bundred, N. Breast carcinoma: Vascular density determined using CD105 antibody correlates with tumor prognosis. *Cancer Res.* **1999**, *59*, 856–861.

27. Li, C.; Gardy, R.; Seon, B.K.; Duff, S.E.; Abdalla, S.; Renehan, A.; O'Dwyer, S.T.; Haboubi, N.; Kumar, S. Both high intratumoral microvessel density determined using CD105 antibody and elevated plasma levels of CD105 in colorectal cancer patients correlate with poor prognosis. *Br. J. Cancer* **2003**, *88*, 1424–1431. [CrossRef]

28. Salvesen, H.B.; Gulluoglu, M.G.; Stefansson, I.; Akslen, L.A. Significance of CD 105 expression for tumour angiogenesis and prognosis in endometrial carcinomas. *APMIS* **2003**, *111*, 1011–1018. [CrossRef]

29. Kyzas, P.A.; Agnantis, N.J.; Stefanou, D. Endoglin (CD105) as a prognostic factor in head and neck squamous cell carcinoma. *Virchows Arch.* **2006**, *448*, 768–775. [CrossRef]

30. Zvrko, E.; Mikic, A.; Vuckovic, L.; Djukic, V.; Knezevic, M. Prognostic relevance of CD105-assessed microvessel density in laryngeal carcinoma. *Otolaryngol. Head. Neck Surg.* **2009**, *141*, 478–483. [CrossRef]

31. Schimming, R.; Marmé, D. Endoglin (CD105) expression in squamous cell carcinoma of the oral cavity. *Head. Neck* **2002**, *24*, 151–156. [CrossRef] [PubMed]

32. Chien, C.Y.; Su, C.Y.; Hwang, C.F.; Chuang, H.C.; Chen, C.M.; Huang, C.C. High expressions of CD105 and VEGF in early oral cancer predict potential cervical metastasis. *J. Surg. Oncol.* **2006**, *94*, 413–417. [CrossRef] [PubMed]

33. Marioni, G.; Marino, F.; Giacomelli, L.; Staffieri, C.; Mariuzzi, M.L.; Violino, E.; De Filippis, C. Endoglin expression is associated with poor oncologic outcome in oral and oropharyngeal carcinoma. *Acta Otolaryngol.* **2006**, *126*, 633–639. [CrossRef]

34. Marioni, G.; Staffieri, A.; Fasanaro, E.; Stramare, R.; Giacomelli, L.; Bernardi, E.; Val, M.; Stellini, E.; de Filippis, C.; Blandamura, S. The role of angiogenin in pT1-T2 tongue carcinoma neo-angiogenesis and cell proliferation: An exploratory study. *J. Oral Pathol. Med.* **2013**, *42*, 606–611. [CrossRef] [PubMed]

35. Martone, T.; Rosso, P.; Albera, R.; Migliaretti, G.; Fraire, F.; Pignataro, L.; Pruneri, G.; Bellone, G.; Cortesina, G. Prognostic relevance of CD105+ microvessel density in HNSCC patient outcome. *Oral Oncol.* **2005**, *41*, 147–155. [CrossRef] [PubMed]

36. Lionello, M.; Staffieri, A.; Marioni, G. Potential prognostic and therapeutic role for angiogenesis markers in laryngeal carcinoma. *Acta Otolaryngol.* **2012**, *132*, 574–582. [CrossRef]

37. Lovato, A.; Marioni, G.; Manzato, E.; Staffieri, C.; Giacomelli, L.; Ralli, G.; Staffieri, A.; Blandamura, S. Elderly patients at higher risk of laryngeal carcinoma recurrence could be identified by a panel of two biomarkers (nm23-H1 and CD105) and pN+ status. *Eur. Arch. Otorhinolaryngol.* **2015**, *272*, 3417–3424. [CrossRef]

38. Han, B.; Lin, S.; Yu, L.J.; Wang, R.Z.; Wang, Y.Y. Correlation of ^{18}F-FDG PET activity with expressions of survivin, Ki67, and CD34 in non-small-cell lung cancer. *Nucl. Med. Commun.* **2009**, *30*, 831–837. [CrossRef]

39. Xing, N.; Cai, Z.L.; Zhao, S.H.; Yang, L.; Xu, B.X.; Wang, F.L. The Use of CT Perfusion to Determine Microvessel Density in Lung Cancer: Comparison with FDG-PET and Pathology. *Chin. J. Cancer Res.* **2011**, *23*, 118–122. [CrossRef]

40. Westerterp, M.; Sloof, G.W.; Hoekstra, O.S.; Ten Kate, F.J.; Meijer, G.A.; Reitsma, J.B.; Boellaard, R.; van Lanschot, J.J.; Molthoff, C.F. 18FDG uptake in oesophageal adenocarcinoma: Linking biology and outcome. *J. Cancer Res. Clin. Oncol.* **2008**, *134*, 227–236. [CrossRef]

41. Groves, A.M.; Shastry, M.; Rodriguez-Justo, M.; Malhotra, A.; Endozo, R.; Davidson, T.; Kelleher, T.; Miles, K.A.; Ell, P.J.; Keshtgar, M.R. 18F-FDG PET and biomarkers for tumour angiogenesis in early breast cancer. *Eur. J. Nucl. Med. Mol. Imaging* **2011**, *38*, 46–52. [CrossRef]

42. Cochet, A.; Pigeonnat, S.; Khoury, B.; Vrigneaud, J.M.; Touzery, C.; Berriolo-Riedinger, A.; Dygai-Cochet, I.; Toubeau, M.; Humbert, O.; Coudert, B.; et al. Evaluation of breast tumor blood flow with dynamic first-pass 18F-FDG PET/CT: Comparison with angiogenesis markers and prognostic factors. *J. Nucl. Med.* **2012**, *53*, 512–520. [CrossRef]

43. Goh, V.; Rodriguez-Justo, M.; Engledow, A.; Shastry, M.; Endozo, R.; Peck, J.; Meagher, M.; Taylor, S.A.; Halligan, S.; Groves, A.M. Assessment of the metabolic flow phenotype of primary colorectal cancer: Correlations with microvessel density are influenced by the histological scoring method. *Eur. Radiol.* **2012**, *22*, 1687–1692. [CrossRef]

44. Surov, A.; Meyer, H.J.; Gawlitza, M.; Höhn, A.K.; Boehm, A.; Kahn, T.; Stumpp, P. Correlations Between DCE MRI and Histopathological Parameters in Head and Neck Squamous Cell Carcinoma. *Transl. Oncol.* **2017**, *10*, 17–21. [CrossRef]

45. Ash, L.; Teknos, T.N.; Gandhi, D.; Patel, S.; Mukherji, S.K. Head and neck squamous cell carcinoma: CT perfusion can help noninvasively predict intratumoral microvessel density. *Radiology* **2009**, *251*, 422–428. [CrossRef]